Icarus 206 (2010) 95–103

Contents lists available at ScienceDirect

Icarus

journal homepage: www.elsevier.com/locate/icarus

Radar absorption due to a corotating interaction region encounter with Mars detected by MARSIS

David D. Morgan [a,*], Donald A. Gurnett [a], Donald L. Kirchner [a], J. David Winningham [b], Rudy A. Frahm [b], David A. Brain [c], David L. Mitchell [c], Janet G. Luhmann [c], Erling Nielsen [e], Jared R. Espley [d], Mario H. Acuña [d,1], Jeffrey J. Plaut [f]

[a] Department of Physics and Astronomy, The University of Iowa, Iowa City, IA 52242, USA
[b] Southwest Research Institute, San Antonio, TX 78228, USA
[c] Space Science Laboratory, University of California, Berkeley, CA 94720, USA
[d] NASA Goddard Space Flight Center, Greenbelt, MD 20771, USA
[e] Max Plank Institute for Solar System Research, Katlenburg-Lindau, D-37191, Germany
[f] Jet Propulsion Laboratory, Pasadena, CA 91109, USA

ARTICLE INFO

Article history:
Received 15 October 2008
Revised 26 February 2009
Accepted 4 March 2009
Available online 14 March 2009

Keywords:
Mars
Ionospheres
Solar wind
Radar observations

ABSTRACT

Mars Advanced Radar for Subsurface and Ionospheric Sounding (MARSIS) is a subsurface and topside ionosphere radar sounder aboard the European Space Agency spacecraft Mars Express, in orbit at Mars since 25 December 2003, and in operation since 17 June 2005. The ionospheric sounding mode of MARSIS is capable of detecting the reflection of the sounding wave from the martian surface. This ability has been used in previous work to show that the surface reflection is absorbed and disappears during periods when high fluxes of energetic particles are incident on the ionosphere of Mars. These absorption events are believed to be the result of increased collisional damping of the sounding wave, caused by increased electron density below the spacecraft, in turn caused by impact ionization from the impinging particles. In this work we identify two absorption events that were isolated during periods when the surface reflection is consistently visible and when Mars is nearly at opposition. The visibility of the surface reflection is viewed in conjunction with particle and photon measurements taken at both Mars and Earth. Both absorption events are found to coincide with Earth passing through solar wind speed and ion flux signatures indicative of a corotating interaction region (CIR). The two events are separated by an interval of approximately 27 days, corresponding to one solar rotation. The first of the two events coincides with abruptly enhanced particle fluxes seen *in situ* at Mars. Simultaneous with the particle enhancement there are an abrupt decrease in the intensity of electron oscillations, typically seen by the Mars Express particle instrument ASPERA-3 between the magnetic pileup boundary and the martian bow shock, and a sharp drop in the solar wind pressure, seen in the proxy quantity based on MGS magnetometer observations. The decrease in oscillation intensity is therefore the probable effect of a relaxation of the martian bow shock. The second absorption event does not show a particle enhancement and complete ASPERA-3 data during that time are unavailable. Other absorption events are the apparent result of solar X-ray and XUV enhancements. We conclude that surface reflection absorption events are sometimes caused by enhanced ionospheric ionization from high energy particles accelerated by the shocks associated with a CIR. A full statistical analysis of CIRs in relation to observed absorption events in conjunction with a quantitative analysis of the deposition of ionization during space weather events is needed for a complete understanding of this phenomenon. If such analyses can be carried out, radar sensing of the martian ionosphere might be useful as a space weather probe.

1. Introduction

The Mars Advanced Radar for Subsurface and Ionospheric Sounding (MARSIS), aboard the ESA spacecraft Mars Express, was deployed on 17 June 2005, one year and six months after Mars Express was inserted into orbit on 25 December 2003, and over two years after Mars Express was launched on 2 June 2003. The instru-

* Corresponding author. Fax: +1 (319) 335 1753.
E-mail address: avid-morgan@uiowa.edu (D.D. Morgan).
[1] Deceased March 5, 2009.

0019-1035/$ - see front matter © 2009 Elsevier Inc. All rights reserved.
doi:10.1016/j.icarus.2009.03.008

ment rapidly bore scientific fruit, both in its subsurface mode (Picardi et al., 2005; Plaut et al., 2007) and in its Active Ionospheric Sounder (AIS) mode (Gurnett et al., 2005, 2008). It was noted that at times the reflection of the sounding wave from the surface of Mars can be detected by MARSIS in ionospheric sounding mode. Morgan et al. (2006) state that this was usually the case when the spacecraft was sampling at solar zenith angles greater than about 50°, an effect noted and modeled by Nielsen et al. (2007). Morgan et al. (2006) also identified five periods between July and September of 2005 when the spacecraft was at high solar zenith angle and the surface reflection was absorbed. (The existence of these absorption events was confirmed by Espley et al., 2007, using MARSIS in subsurface mode to detect the surface reflection.) The study by Morgan et al. (2006) concluded that these prolonged absorption events coincided with enhanced fluxes of energetic particles, probably $\geqslant$10 MeV protons, similar to polar cap absorption events (PCAs) observed in the Earth's Antarctic (Bailey, 1964; Patterson et al., 2001). These events also meet the description of a gradual proton event (GPE), comprising high energy particles that accompany a coronal mass ejection (CME). GPEs at Mars are treated theoretically by Leblanc et al. (2002). The impinging energetic particles are believed to cause impact-ionization of CO_2, increasing the electron density in the martian ionosphere, and causing collisional damping of radio waves. The theory of collisional damping of radio waves is given by Gurnett and Bhattacharjee (2005).

The effect of energetic particles in the atmosphere and ionosphere of Mars is one of both intrinsic and practical interest. For example, the images from the MARSIS Subsurface Sounder are degraded and sometimes obliterated when the ionization is increased by impinging energetic particles (Espley et al., 2007). More recently, Dubinin et al. (2009) have detected a corotating interaction region at Mars using ASPERA-3 electron and ion data in conjunction with *in situ* electron densities taken by MARSIS (see Duru et al., 2008 for an explanation of these data). These authors emphasize the role of space weather events in eroding plasma from the martian ionosphere. Because the visibility of the surface reflection is a rough gauge of the total number of electrons along the ray path of the sounding pulse, it might be used in conjunction with atmospheric and ionospheric models to obtain a quantitative profile of particle energy deposition in the martian ionosphere. Such information would have implications for the possibility of development of life on the martian surface and for the safety of human beings in orbit or at the the surface of Mars. However, such a quantitative analysis is in the future and beyond the scope of the present paper.

The orbit of Mars is located in a region of interplanetary space where space weather events are at varying stages of development. It may be possible to use radar sensing of the martian ionosphere to sense these events and gauge their state of evolution. Such an application will depend on a more thoroughgoing multi-instrument statistical analysis than is presented here. In any case, we would like to describe the causes and effects of energetic particle events at Mars in as much detail as possible, for a wide variety of applications.

Radio wave absorption at Mars and the related topic of solar effects on the electron density profile in the martian ionosphere are the subject of several other studies. Nielsen et al. (2007) model radio wave absorption in the martian atmosphere and reproduce the observed decrease in attenuation with increasing solar zenith angle. Espley et al. (2007), using the MARSIS subsurface mode to probe the absorption properties of the martian ionosphere, confirm that the subsurface absorption events largely coincide with those detected by the ionospheric sounder and with solar energetic particle enhancements. Wang and Nielsen (2004) demonstrate that solar wind protons of energy $\sim$1 MeV influence the peak altitude of electron density in the martian ionosphere through heating and ionization. Gurnett et al. (2005) show an example of a solar flare directly enhancing the maximum detected plasma frequency. Mendillo et al. (2006) use the MGS Radio Occultation experiment to generate electron density profiles due to ionization from the X-ray component of a solar flare. Leblanc et al. (2002) predict the effectiveness of high energy particles from X-ray enhancements, gradual proton events, and corotating interaction regions (CIRs).

The purpose of this paper is to show the probable relation of some MARSIS absorption events with CIRs. A CIR occurs when a region of high speed solar wind, originating in a region of low XUV and X-ray intensity called a coronal hole, comes in contact with a leading stream of slow solar wind. At heliospheric distances of about 0.5 AU, the magnetic field, frozen into the Parker spiral, becomes oblique enough to the solar wind, flowing in a primarily radial direction, to cause compressional effects to determine the structure of the boundary between the two streams. This structure, including the development of forward and reverse shocks, becomes stable at 2–4 AU, beyond the orbit of Mars (Balogh et al., 1999; Crooker et al., 1999). However, this range of distances is not ironclad; in about 20% of cases, a reverse shock at the trailing edge of a CIR can be observed near Earth (Tsurutani et al., 2006). The shocks associated with CIRs are capable of accelerating ions in the interplanetary medium to MeV energies. Coronal holes and their corresponding CIRs can be stable over several solar rotations. The relation of CIRs to geomagnetic activity at Earth is reviewed by Tsurutani et al. (2006). The development of CIRs and their accompanying forward and reverse shocks are discussed by Balogh et al. (1999) and Crooker et al. (1999).

While Morgan et al. (2006) were able to associate absorption intervals with particle enhancements, the level of solar activity during that epoch made it hard to relate them to observations of the interplanetary medium made from Earth orbit. In this study, we initially consider an event on December 1–2, 2005, that is isolated from other events, creating an opportunity to study associated observations at Earth without the complication caused by observations of overlapping particle and radiative events of various types. We use particle, solar wind, and magnetic field measurements made at Earth and Mars to analyze this absorption event. In addition, we note a similar event occurring approximately one solar rotation subsequent to the original event. We show that this class of absorption event is probably related to the occurrence of fast solar wind and high fluxes of energetic ions characteristic of CIRs.

2. Data

The basic unit of data of the MARSIS ionospheric sounder is called an ionogram, of which a description is given by Morgan et al. (2008). Ionograms are generated every 7.543 s. Each ionogram consists of the color coded map of received radio intensity as a two-dimensional function of 160 frequencies, between 0.125 and 5.5 MHz, and 80 send-receive (or "delay") times, between 0.25 and 7.58 ms. Sample ionograms are given by Gurnett et al. (2005, 2008) and by Morgan et al. (2006, 2008). A useful construct called the "apparent range," i.e., the *inferred* distance from the instrument to the point of reflection assuming wave propagation in a vacuum, can be computed from the delay time by the formula $z_{app} = ct_{delay}/2$; here, z_{app} is the apparent range (*not* altitude), t_{delay} the time delay, and c the vacuum speed of light.

A feature that is frequently seen in MARSIS ionograms is the reflection of the sounding wave from the surface of the planet. Excellent examples of MARSIS surface reflection traces can be seen in Figs. 2 and 7 of the review by Gurnett et al. (2008). The defining characteristic of the surface reflection is that the apparent range asymptotically approaches the altitude of the spacecraft with increasing frequency due to the decreasing effect of plasma dispersion. The theory of this phenomenon is reviewed by Morgan et al. (2006).

Fig. 1 shows ionograms from the available orbits before, during, and after an absorption event observed on 1–2 December 2005.

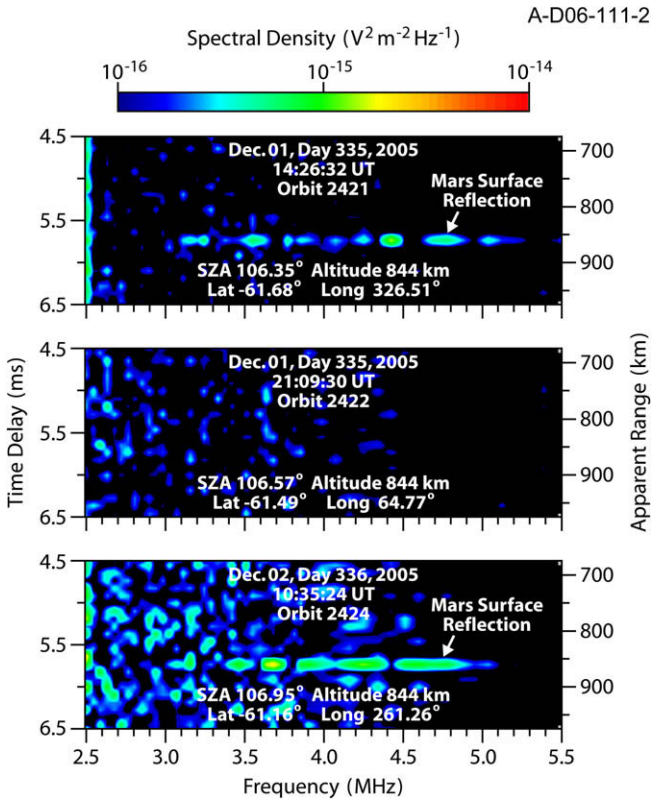

Fig. 1. Sample ionograms before, during, and after the absorption event of 1–2 December 2005. The horizontal axis corresponds to the frequency of the sounding wave. The vertical axis corresponds to the delay time, as marked on the left, or equivalently, the apparent range, as marked on the right of each ionogram. The color coding of the display corresponds to the reflected wave intensity. The Mars surface reflection signal, if visible, should appear at an apparent altitude approaching 850 km from greater values at increasing frequencies. (Top) Ionogram near altitude 850 km on the inbound leg of orbit 2421. The surface reflection is plainly visible at frequencies greater than 3 MHz. (Middle) Ionogram near altitude 850 km on the inbound leg of orbit 2422. The surface reflection is not visible. (Bottom) Ionogram near altitude 850 km on the inbound leg of orbit 2424. The surface reflection is plainly visible. The diffuse brightening at low frequency is the result of a solar Type III radio event, unrelated to the absorption event under study. Longitude is given in degrees west, latitude in degrees north.

The top panel shows an ionogram near 850 km altitude on the inbound leg of orbit 2421, prior to the event under study. In this figure, the sounding frequency is given as the horizontal axis, the time delay as the left-hand side vertical axis, the apparent range as the right-hand side vertical axis, and the received spectral density as the color. The surface reflection is clearly visible as a bright line at apparent range near the spacecraft altitude of 844 km. Because the electron density is low where Fig. 1 is taken, there is little dispersion and the surface reflection is seen as a nearly horizontal line. The middle panel of Fig. 1 shows an ionogram taken at nearly the same altitude and solar zenith angle for orbit 2422. In contrast to the top panel, no surface reflection is visible. Finally, the bottom panel shows an ionogram taken at a similar altitude on orbit 2424 (the next available); here, the surface reflection has reappeared.

We have tabulated, for ionograms collected through most of the spacecraft mission, the surface reflection visibility, given as a zero when the surface reflection is not visible, and a one, when the surface reflection is visible. The two workers who performed the tabulation were both trained to record as visible any trace distinguishable from background and recognizable as a surface reflection, no matter how faint. The advantage of this method is that there are very few cases where there is any room for error; in almost all cases the surface reflection is either clearly visible or not visible at all. Ionograms were displayed for examination using a single standard color bar. The evaluations of visibility of the two workers were checked for consistency.

The statistical technique used in this and previous work is to sample the surface reflection visibility for ten ionograms nearest a given altitude and take the average, a process that yields a data point once per orbit, or approximately once every 7 h. This procedure has been followed at altitudes of 850 and 1050 km and at periapsis, approximately 275 km. Because each orbit has inbound and outbound legs, this sampling technique gives us five tries at acquiring data at solar zenith angles greater than 50° sampled at a frequency of 1 sample every two orbits, i.e., 1/14 h or greater. For Figs. 2 and 3, only the inbound leg at altitudes of 850 and 1050 km meet these two criteria.

Fig. 2 shows the averaged surface reflection in conjunction with related observations taken from both Mars and Earth orbit. Panel 1 shows the averaged surface reflection visibility at altitude 850 km and 1050 km as a function of time. These averages are taken from the inbound leg of each orbit; the outbound leg did not meet criteria for solar zenith angle and sampling frequency. The Subsurface Sounder surface reflection visibility at periapsis, as tabulated by Espley et al. (2007), is also plotted on this panel. All three indices indicate an abrupt absorption event that takes place during orbit 2422, on DOY 335–336 (December 1–2), 2005. Onset and recovery times with estimated uncertainties are given in the figure. The uncertainty on the recovery phase is twice as long as on the onset because there is no sample during the orbit immediately following the absorption onset.

Panel 2 shows the background count rate of the Mars Global Surveyor Electron Reflectometer (MGS ER) during the time of this event. These data are smoothed over a period of two hours, the orbital period of MGS. Only the highest-energy channel, at 18.2 keV, is sampled, since it should contain the highest proportion of background counts, indicative of MeV-energy ions that are capable of penetrating the instrument shielding. The error bar shown by dashed lines is the standard deviation on the smoothed count rates over the entire interval. Note that there is an abrupt increase in the background count rate that peaks at $\sim 2\sigma$ above normal, coincident with the absorption event seen by both ionospheric and subsurface modes of MARSIS. The duration of this enhancement, between 18:34 UT on day 335 through 03:00 UT on day 336, is shown bracketed by vertical dotted lines.

Panel 3 of Fig. 2 shows the subsolar solar wind pressure, with uncertainty, computed from MGS MAG/ER data, as explained by Crider et al. (2003). A large spike in solar wind pressure precedes the absorption event by approximately two days. It is not clear whether this pressure spike is related to the absorption event. Following the peak and starting about day 335 there is a plateau followed by an abrupt drop in solar wind pressure (bracketed by dotted lines), nearly coinciding with the onset of the particle enhancement shown in Panel 2.

Panel 4 of Fig. 2 shows the subsolar magnetic field (dots, labeled at left) based on the same MGS magnetometer measurements used for the pressure proxy shown in Panel 3. The magnetic field measured by the magnetometer on the Advanced Composition Explorer (ACE) spacecraft in Earth orbit (lines, labeled at right) is also shown. The MGS magnetic field has a maximum near day 335, followed by a period of enhanced magnetic field, corresponding to the plateau in pressure shown in Panel 3. The ACE magnetometer measurements have a similar structure peaking near day 334. The corresponding peaks are shown by vertical dotted lines. The similarity of these structures at Earth and Mars suggest that they represent the same event intersecting the orbits of the two planets. Under this assumption, a time of flight velocity of 741 ± 53 km/s can be calculated.

Panel 5 of Fig. 2 shows the intensity of 1.91–4.75 MeV ions detected by the Electron, Proton, and Alpha Monitor (EPAM) instru-

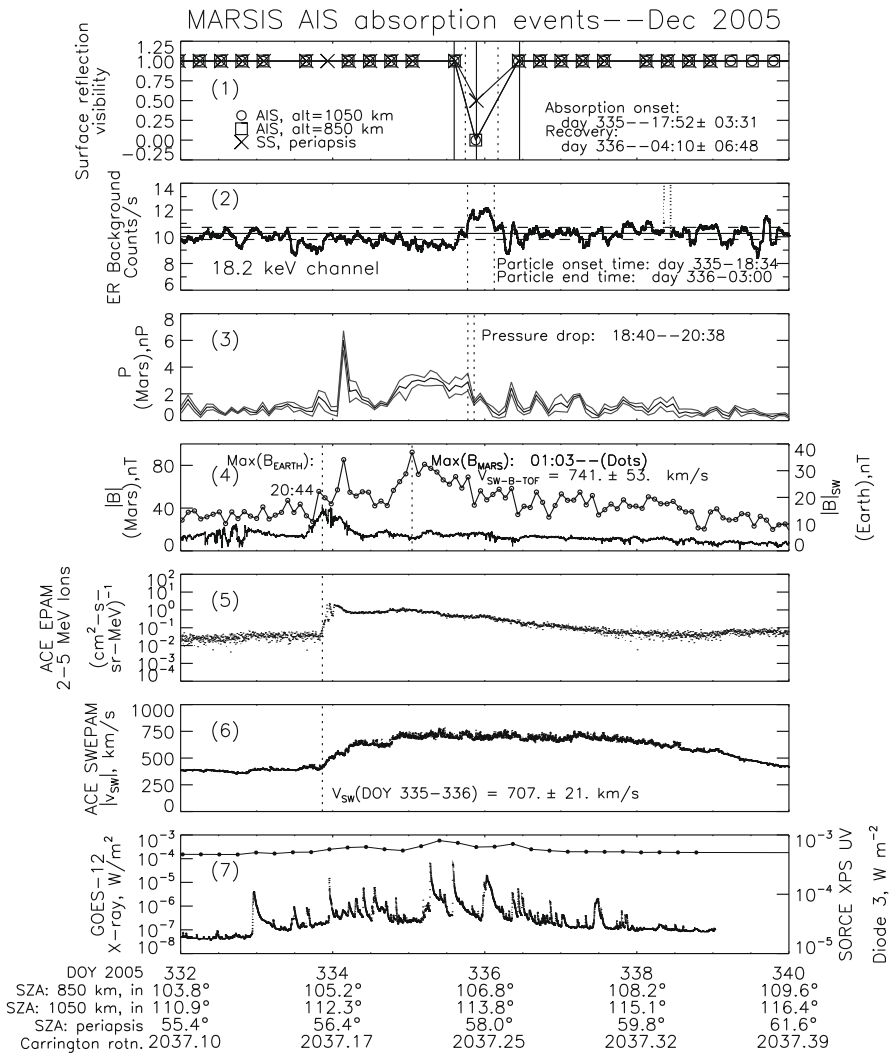

Fig. 2. The radar absorption event of 1–2 December 2005 with accompanying data. (1) MARSIS surface reflection visibility. Open circles represent the surface reflection visibility averaged for ten ionospheric sounder ionograms nearest an altitude of 1050 km. Open squares represent the same quantity at 850 km. Diagonal crosses represent the surface reflection quality from the MARSIS subsurface mode as indexed by Espley et al. (2007). Values of one indicate that the surface is clearly visible; values of zero indicate that it is completely obscured. The onset time is computed to be 17:52 UT ± 3.5 h. (2) Two-hour-smoothed MGS ER background counts in the 18.2 keV channel. There is a weak enhancement between day 335 18:34 and day 336 03:00, determined as the time when the count rate is 1σ above average background. We cite these times with an uncertainty of 2 h corresponding to the orbital period of MGS. Both onset of and recovery from the absorption event coincide with the absorption observed in the top panel. (3) Solar wind pressure proxy generated from MGS magnetometer measurements as explained by Crider et al. (2003), with uncertainties shown. The large spike on day 334 is not clearly associated with the absorption event on days 335–336. However, a plateau in the pressure starting near day 335 is followed by a distinct drop-off coinciding with the particle onset shown in Panel 2. (4) Subsolar magnetic field magnitude from the MGS magnetometer. The absorption event is preceded by two sharp increases in the solar wind pressure at approximately two days and eighteen hours before absorption onset (connected dots, labeled at left). Also plotted, the magnetometer data acquired from ACE in Earth orbit (lines, labeled at right). An increase in the Earth-based magnetic field on day 333 20:44 UT is mirrored by a similar increase on day 335 at 01:03 UT. The peaks in magnetic field at Earth and Mars (shown by vertical dotted lines) are used to compute a time-of-flight estimate of the speed of propagation. (5) Flux of 1.91–4.75 MeV ions from the EPAM instrument aboard ACE in Earth orbit. An abrupt onset of ion flux is detected coincident with the peak in magnetic field at day 333 at 20:44 UT. (6) The solar wind speed from ACE SWEPAM in Earth orbit. The solar wind speed increases by almost a factor of two over the course of a day starting with the magnetic peak and particle onset noted in Panels 4 and 5. (7) The soft X-ray flux measured by the solar environment monitor aboard the GOES-12 spacecraft (indicated by small dots and labeled at left). Overplotted is the XUV intensity detected at Earth by Diode 3 of the XPS instrument aboard the SORCE spacecraft (indicated by large dots and labeled at right) at 24 h intervals. The times are corrected by the solar rotation time corresponding to the azimuthal angle between Earth and Mars. The absorption and particle events shown in the top two panels occur while both X-rays and XUV are enhanced.

ment aboard ACE. There is an abrupt increase in particle intensity on day 333 (29 November) at 22:02 UT followed by an abrupt decrease and then a slow decrease (roughly an order of magnitude every two days) back toward the original intensity.

Panel 6 shows the solar wind speed, measured by the Solar Wind EPAM (SWEPAM) aboard ACE, rising from about 400 to 700 km/s over about a day. The start of this increase coincides with the particle burst observed in the third panel.

The changes in particle flux and solar wind speed shown in Panels 5 and 6 are typical signatures of a CIR (see, Tsurutani et al., 2006). Because the CIR is embedded in the solar wind, the radial component of its motion should be that of the solar wind. In Panel 6 we have taken an average of the solar wind speed around its maximum, which gives a value of 707 ± 21 km/s. This value is consistent with the time-of-flight velocity computed from the peak magnetic fields in Panel 4.

Panel 7 shows radiative fluxes at two wavelengths: the 0.1–0.8 nm X-ray flux measured by GOES-12 (indicated by small dots and labeled at left), and 24 h averages of the ultraviolet radiation in the range of 17 to 23 nm (indicated by connected large dots and labeled at right), measured by Diode 3 of the Extreme Ultraviolet Photometer System (XPS) aboard the Solar Radiation and Climate Experiment (SORCE) spacecraft. Both detectors are in Earth orbit. Both fluxes are plotted against time corrected by the solar rotation

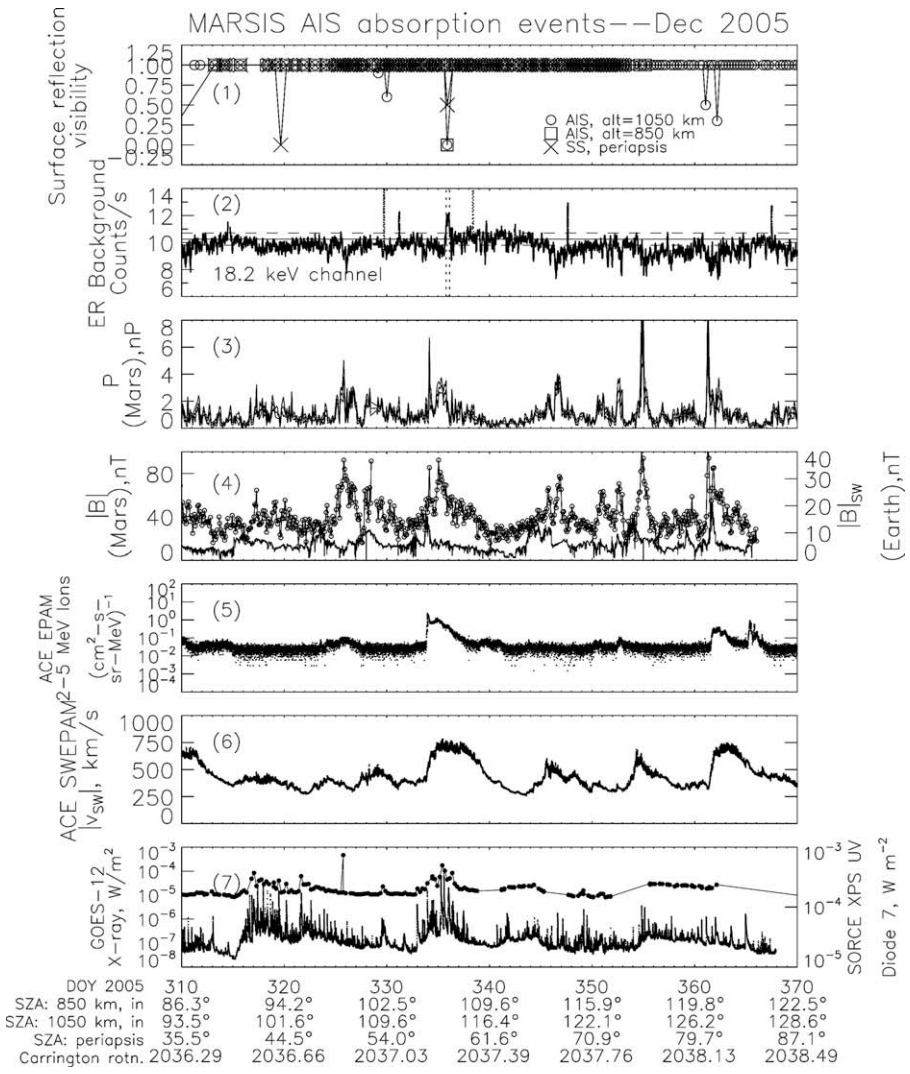

Fig. 3. The same quantities as in Fig. 2 but for an expanded time and using Diode 7, which is available as 6 h averages, instead of Diode 3. There are two absorption events near day 360, roughly one solar rotation later than the event on day 335, shown in the previous plot, and shown toward the center here. These two events correspond with solar wind speed, high energy particle, and magnetic features that are very similar to those seen at day 335. There is no *in situ* particle enhancement visible, probably because the particles causing ionospheric absorption were not energetic enough to penetrate the shielding of MGS ER. There are no enhancements in X-ray or XUV flux that might explain the two absorptions. Absorption events seen earlier than day 335 may be explained by X-ray–EUV enhancements.

time corresponding to the azimuthal angle between Earth and Mars. The absorption event noted in the top two panels occurs during an increase in both XUV and X-ray flux, indicating that a region of high irradiance was rotating into view at Mars when the absorption event happened. Therefore, a radiative contribution to the December 1–2, 2005 event is possible. An increase in electron density in the martian ionosphere due to solar active regions rotating into view is demonstrated by Withers and Mendillo (2005) using electron density profiles from the MGS radio occultation experiment.

The data plotted in Fig. 3 are almost the same as shown in Fig. 2 but expanded to include the next Carrington rotation. (The XUV flux plotted in Panel 6 is now taken from XPS diode 7 at 0.1–0.7 nm with averages given at 6 h intervals instead of 24 h intervals, since the longer wavelength flux from diode 3 ends at day 353.) This widened comparison indicates two absorption events coinciding with solar wind speed and particle flux increases measured at Earth during Carrington rotation 2038, near day 360. Panels 3 and 4 reveal that the absorption events near day 360 are associated with pressure and magnetic field structures similar to those encountered for the event on day 335. The Earth-based ion and solar wind speed signatures of the two events are also similar. The two events differ in that MGS MAG/ER does not detect an *in situ* particle flux increase during the latter events; however, neither is there a solar radiation enhancement that can explain this absorption feature.

There are also absorption events earlier in this interval, near day 320 and 330. The event near day 320 is seen only in the subsurface visibility. It does not correspond to particle episodes observed at Earth. It does appear to coincide with the maximum of an X-ray region as it rotates into view at both Earth and Mars. The event near day 330 consists of two weak absorption episodes in the surface reflection visibility taken at 1050 km altitude that also do not correspond to high values of either solar wind or ion flux. This absorption event coincides roughly with a weak but relatively long-lived X-ray flare. These events may be examples of MARSIS absorption caused by photons without the participation of particle fluxes.

The next solar rotation periods (Carrington 2039, 2040) include a number of absorption events that may be attributed to either particle or radiative causes, but the evolving shape of the solar wind and particle structures and the worsening alignment of Earth and Mars make these events hard to correlate with solar wind and radiation data; therefore, we do not show them.

Fig. 4 shows observations, coinciding with the MARSIS absorption event of 1–2 December 2005, by the Analyzer of Space Plasmas and

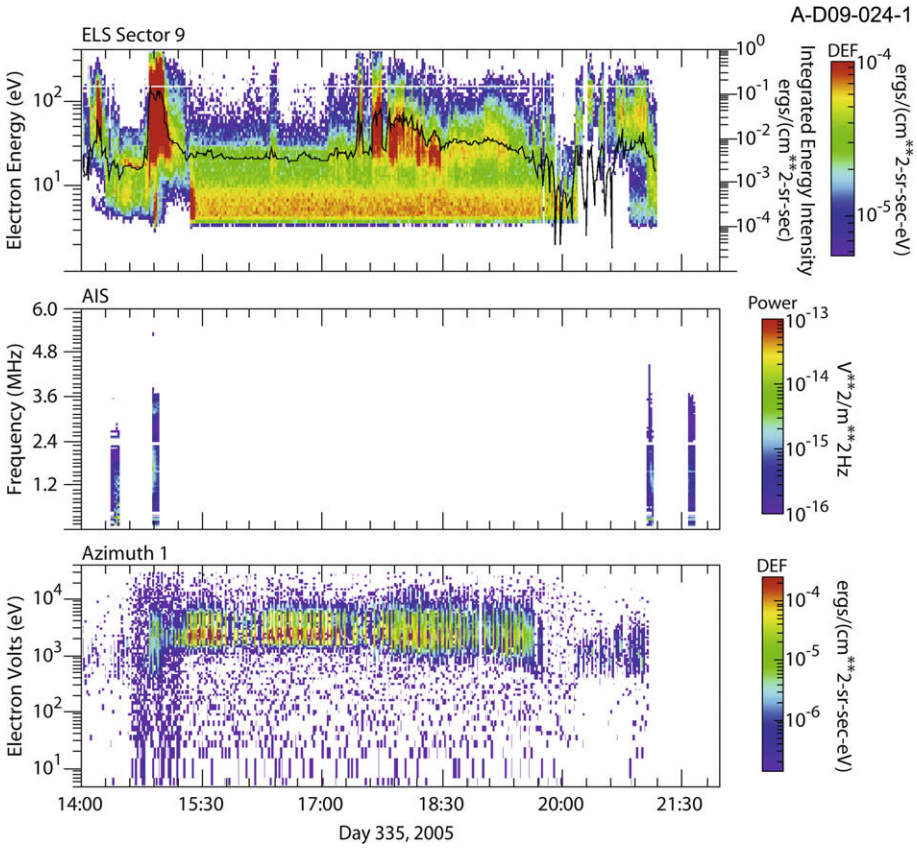

Fig. 4. ASPERA-3 and MARSIS ionospheric sounder data plotted together in spectrogram form. (Top) ASPERA-3 electron spectrometer (ELS) differential energy fluxes (DEF) color-plotted as a function of universal time (horizontal axis) and electron energy (left-hand vertical axis). The black line through the DEF data is the integral energy intensity, labeled and scaled on the right-hand vertical axis. Sector 9 refers to one of sixteen electron analyzers on the instrument. Electron oscillations are observed from 17:00 to 19:30 UT, during which time Mars Express is in the solar wind. The reduced oscillation intensity at 18:30 UT may be due to an abrupt relaxation of the martian bow shock, indicated by the simultaneous pressure drop seen in the MGS pressure proxy in Panel 3 of Fig. 3. The intensity decease in electron oscillation also coincides with the particle increase detected by the MGS Electron Reflectometer. (Middle) MARSIS ionospheric sounder intervals are shown to indicate timing of the inbound and outbound legs of orbits 2421 and 2422. The absorption event occurs on the inbound leg of orbit 2422 at about 21:08 UT on day 335. (Bottom) ASPERA-3 Ion Mass Analyzer (IMA) data, showing a slight broadening of the ion energy bandwidth at the same time that the electron oscillations are observed in the top panel.

Energetic Ions (ASPERA-3, see Barabash et al., 2004), on board Mars Express. (Complete ASPERA-3 data were not available for the events of 26–28 December 2005.) The top panel shows electron energy flux, detected by the ASPERA-3 electron spectrometer (ELS). The high fluxes below 10 eV occur when Mars Express is immersed in solar wind plasma. Between 17:20 and 19:30 UT and at energies above 10 eV, there are high electron fluxes known to be due to electron oscillations, as explained by Espley et al. (2004) and Winningham et al. (2006). These authors showed that these oscillations are caused by ion cyclotron instabilities and are present in the region between the bow shock and the MPB at all times. The intensity of the electron oscillations undergoes fluctuation in intensity between 17:10 UT and 18:30 UT. There is a sharp decrease in oscillation intensity at 18:30 UT, followed by faint but steady oscillation strength. The observed decrease in oscillation strength is nearly simultaneous with the onset, at 18:34 UT, of the enhanced background event observed by the MGS Electron Reflectometer on 1–2 December 2005, as well as the solar wind pressure drop detected by the MGS magnetometer pressure proxy at 18:40 UT. The middle panel of Fig. 4 shows the timing of the MARSIS observations. Orbit 2421 is represented by the vertical blue stripes at left and orbit 2422, the orbit of the absorption event, by those at right. The third panel of Fig. 4 shows ion energy flux detected by the ASPERA-3 Ion Mass Analyzer (IMA) during this period. The ion flux appears to increase and then decrease in concert with the electrons.

Because the duration of the MGS Electron Reflectometer particle enhancement closely brackets the MARSIS absorption event near 21:05 UT, and because the onset of this particle enhancement so closely coincides with the decrease in electron oscillation intensity detected by ASPERA-3 ELS, we believe it is likely that the decrease in oscillation intensity, the enhancement in Electron Reflectometer background counts, and the absorption of the surface reflection observed by MARSIS are all caused by the same solar wind event, commencing at about 18:30 UT on 1 December 2005. Because these events also coincide closely with the abrupt drop in solar wind pressure at 18:40 UT, we think it likely that these events are best explained by the occurrence of a reverse shock associated with a CIR.

Fig. 5 shows the orbit of Mars Express during and slightly before Orbit 2422. The position of MARSIS during the ASPERA-3 data interval, shown in Fig. 4, at the time the intensity of the electron oscillations decreases, and during the MARSIS data collection interval. The reduction in intensity of the electron oscillations occurs when Mars Express is midway between the quiet-time positions of the martian bow shock and the magnetic pileup boundary, both based on the computations of Vignes et al. (2000). The MARSIS absorption event is observed about 2.5 h later, with Mars Express near periapsis. The bow shock appears to have abruptly relaxed around 18:30 UT, causing an expansion of the cavity in which the oscillations occur and therefore reducing their intensity.

We have examined radar absorption data during the following time interval when Mars is near opposition, which occurred between December 2007 and February 2008. Although MARSIS absorption events are seen at approximately 27 day intervals and

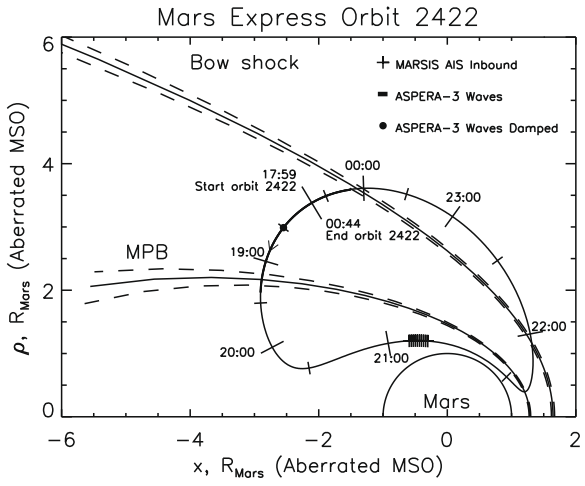

Fig. 5. Mars Express Orbit 2422, 1–2 December 2005, near to and during the absorption event at 21:08 on 1 December 2005, with Orbit 2421 overlapping from 17:00 to 18:00 UT. The orbits are plotted in cylindrical aberrated Mars Solar Orbital (MSO) coordinates, in which the x-axis is rotated by 4° from the Mars-Sun line to coincide with the oncoming direction of the solar wind. Orbit times at hour intervals (UT) are indicated by tick marks, with half-hours shown with smaller ticks. Mars Express is represented as moving counterclockwise about the orbit path. The inbound portion of Mars Express Orbit 2422, in which the absorption event was observed, is indicated by hash marks just after 21:00 UT. The time interval during which electron oscillations were detected by ASPERA-3 ELS are shown by a thick line and the point at which the waves are seen to be damped is indicated by a large filled circle. This time coincides with the onset of the particle event seen in Panel 2 and the pressure drop-off seen in Panel 3 of Fig. 2. The various coinciding events appear to be best explained by the passage of the reverse shock phase of a CIR.

approximately simultaneous with solar wind velocity enhancements observed by ACE SWEPAM in Earth orbit, the absorption events detected cannot be clearly associated with either particle enhancements observed at Mars or X-ray or XUV radiation enhancements observed from Earth orbit. The source of these later absorption events remains unclear; therefore we do not show them. However, the orbit of Mars is in a region of interplanetary space where CIR-related shocks can be expected to vary in strength, implying that the energetic particles accelerated by these shocks are of varying strength. It is possible that such particles are energetic enough to create ionization in the martian ionosphere without being able to defeat the shielding of the MGS Electron Reflectometer. The ionization response of the martian atmosphere should be modeled to confirm or deny this possibility.

3. Interpretation

Morgan et al. (2006) demonstrated the association of radar absorption events in the martian ionosphere with high energy particles originating at the Sun. To emphasize this point, Fig. 6 shows an expanded segment of Fig. 2 from Morgan et al. (2006), showing the correspondence of radar absorption with high energy particle fluxes detected as background by MGS MAG/ER and Odyssey Gamma Ray Spectrometer. This type of particle event appears to meet the criteria given by Leblanc et al. (2002) for a gradual proton event associated with a coronal mass ejection.

Fig. 2 of the present work indicates the same kind of correspondence between radar absorption and a particle enhancement; however, the events discussed in this paper are different in character from those discussed in the previous work. Instead of being associated with high energy particles originating at the Sun, they coincide most directly with particle and solar wind signatures indicative of CIRs, occurring at intervals roughly equal to that of a solar rotation. Leblanc et al. (2002) also mention CIRs as a possible source of energetic particles at Mars.

The MARSIS absorption event first discussed in this paper, that of 1–2 December 2005, coincides with a visible particle enhancement in the MGS MAG/ER background flux and a rapid drop in solar wind pressure. In Fig. 4, electron oscillations typically seen between the MPB and the martian bow shock undergo an abrupt reduction of intensity simultaneous with the onset of the particle event and pressure drop detected by MAG/ER. The reduced intensity of electron oscillations is apparently associated with an expansion of the bow shock related to the observed pressure decrease, consistent with the passage of the reverse shock phase of a CIR. In this particular case, the absorption event, the particle enhancement, and the pressure drop all occur simultaneously, lending credence to the idea that this event is directly related to the CIR observed at Earth. The decrease in oscillation intensity may be caused by the abrupt expansion of the oscillation cavity.

MARSIS also detected a pair of absorption events approximately one solar rotation period later, around day 360. Although there is no particle enhancement seen in the MGS ER counts, the structural similarity of the various plasma parameters measured at both Earth and Mars indicate the likelihood that this event is also caused by a CIR. The lack of visible high energy particles may be because the energies of the ionizing particles may not be high enough to penetrate the shielding of MGS ER. The absorption event is apparently not due to a solar active region, as indicated by the X-ray flux shown in Fig. 3.

Both absorption events are associated with a spike in the subsolar magnetic field, indicating the probable association of shocks with these CIR crossings. We note that the pressure peaks lead the absorption events in both cases. For this reason, it seems likely that the absorption is caused by energetic particles accelerated by the reverse shock associated with the CIR.

4. Conclusion

Previous work has shown that radar absorption events at Mars can be caused by energetic particles impinging on the martian ionosphere. These absorption events have been shown to coincide precisely with the onset of background enhancements in instruments on two separate spacecraft in orbit about Mars. They are probably identical with those events described by Leblanc et al. (2002) as GPEs, i.e., energetic particles associated with coronal mass ejections. We have now detected absorption events of a different character. The events discussed in this paper are associated with particle and solar wind signatures diagnostic of corotating interaction regions. The two absorption events discussed are separated in time by approximately 27 days, the period of a solar rotation. The first event studied, occurring on 1–2 December 2005, was observed to occur simultaneously with a directly detected particle enhancement and a contraction of the martian bow shock, both typical of an encounter with a CIR. For at least this case, the best explanation appears to be the impinging of energetic particles accelerated by the reverse shock regions associated with the CIR, a phenomenon also predicted by Leblanc et al. (2002). A time-of-flight estimate of the propagation velocity based on magnetic fields measured at Earth and Mars yields a value consistent with the peak solar wind velocity measured at Earth after the CIR onset.

The second absorption event took place about one solar rotation later, about 27 December 2005. This event coincides with ion, solar wind speed, and magnetic signatures that clearly mirror those of the first event. Although we do not directly see energetic particles associated with this event at Mars, the timing of the event, which coincides with the reappearance of the CIR signature in the solar wind and energetic particle observations made at Earth, suggests that the CIR is the cause of the disturbance. It is probable that the energetic particles that cause the absorption are not energetic enough to penetrate the MGS ER shielding and so are invisible to us.

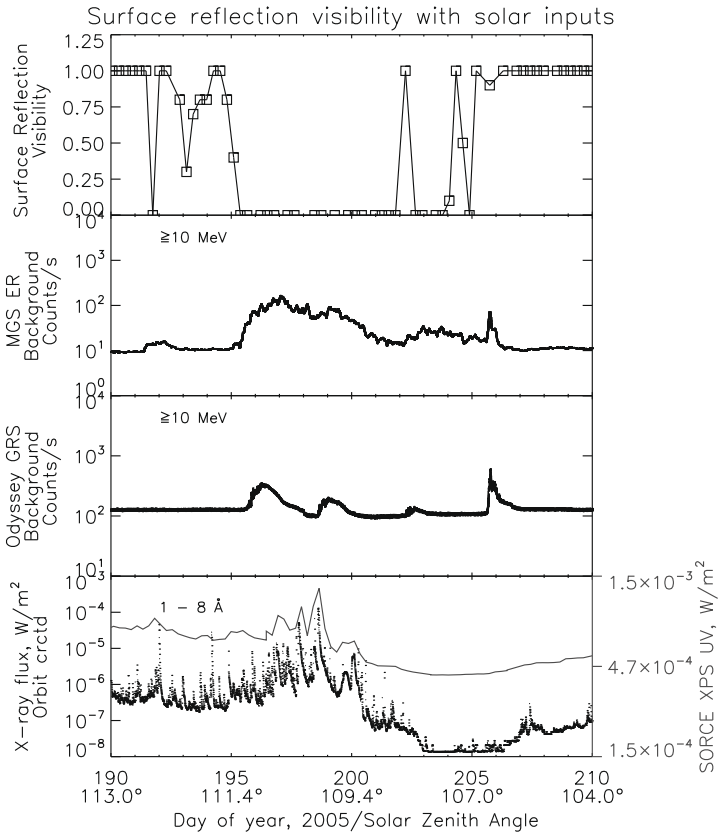

Fig. 6. The panels show absorption event 1 from Morgan et al. (2006). The top panel shows the averaged surface reflection visibility at 850 km altitude for absorption Event 2. The second and third panels show the MGS Electron Reflectometer and the Odyssey Gamma Ray Spectrometer counts during the absorption event. (The reflectometer counts are an average of counts in the 11.2, 14.3, and 18.2 keV channels.) The excess over normal background is presumed to be ions of energy 10 MeV or more, since that is what is required to defeat the instrument shielding. The fourth panel shows X-ray flux as measured by GOES-12 Space Environment Monitor (left-hand vertical axis and small dots) and XUV fluxes, as measured by SORCE XPS (right-hand vertical axis and gray line). The figure shows the close correspondence between the measured particle fluxes and the absorption events. The *X*-axis is labeled with the solar zenith angle at 850 km altitude on the outbound leg of the Mars Express orbit. (Expanded and adapted from Fig. 2 of Morgan et al., 2006.)

During the declining phase of a solar cycle, a CIR striking the martian atmosphere must be common. The forward and reverse shocks, associated with a CIR, and which cause the acceleration of energetic ions observed with CIRs, evolve at heliocentric distances between 0.5 and 2 AU (Crooker et al., 1999). The orbit of Mars, between 1.4 and 1.7 AU, is in the heart of this region of development. It is not surprising that the martian ionosphere would not respond to each passage of a CIR in the same way since different CIR events are likely to pass Mars at different stages of development and therefore accelerate particles to different energies. In the event of 1–2 December 2005 we appear to have encountered an event energetic enough to accelerate particles to energies sufficient to penetrate the shielding of MGS ER. Examination of later sampling periods shows that absorption events are not always detected when CIRs are present, even with Mars near opposition.

In addition, absorption events detected before 1 December, are unrelated to CIRs. These events may be associated with X-ray and XUV active regions at the Sun that are rotating into view at Mars and Earth, although the magnitude and duration of ionization due to such events is not well known. In evaluating radar absorption events at Mars, one must admit that photons have a possible effect, complicating the interpretation of CIR-related absorption events. Nonetheless, in spite of the partial and qualitative nature of our observations, a coincidence of several phenomena point to the action of CIRs introducing enough high energy particles into the ionosphere of Mars to induce absorption of a radar sounding wave. This is an interesting phenomenon in itself; it is interesting that the influence of a mild interplanetary event can be detected low in the ionosphere of Mars. This is also interesting for the designers of remote sensing instruments such as radars and communications devices using radio waves, as it shows that CIRs may interfere with the performance of their instruments. A full understanding of the response of the martian ionosphere to CIRs awaits a comprehensive study utilizing various data sets, for example, MARSIS and ASPERA-3 on Mars Express, MAG/ER on MGS, and various Earth-based instruments, in conjunction with atmospheric and ionospheric modeling efforts. If such a study can be accomplished, our result raises the possibility that the martian ionosphere can be used as a probe of the progress and development of interplanetary events such as CIRs, an idea previously proposed by Withers and Mendillo (2005) with regard to solar radiative flux.

Acknowledgments

We acknowledge the contributions of Ms. Sharon Kutcher, Ms. Zeynep Sagtas Bilki, Mr. Edward West, and Mr. Joe Groene. This work was supported through NASA by JPL Contract 1224107 at the University of Iowa and NASA contract NASW-00003 at Southwest Research Institute.

References

Bailey, D.K., 1964. Polar-cap absorption. Planet. Space Sci. 12, 495–541.
Balogh, A., and 23 colleagues, 1999. The solar origin of corotating interaction regions and their formation in the inner heliosphere. Space Science Rev. 89, 141–178.

Barabash, S., and 47 colleagues, 2004. ASPERA-3: Analyzer of Space Plasmas and Energetic Ions for Mars Express. In: Wilson, A. (Ed.), Mars Express: A European Mission to the Red Planet. ESA Publications Division, ESTEC, Noordwijk, Netherlands, pp. 121–140.

Crider, D.H., Vignes, D., Krymskii, A.M., Breus, T.K., Ness, N.F., Mitchell, D.L., Slavin, J.A., Acuña, M.H., 2003. A proxy for determining solar wind dynamic pressure at Mars using Mars Global Surveyor data. J. Geophys. Res. 108 (A12). doi:10.1029/2003JA009875.

Crooker, N.U., and 21 colleagues, 1999. CIR morphology, turbulence, discontinuities, and energetic particles. Space Science Rev. 89, 179–220.

Dubinin, E., Fraenz, M., Woch, J., Duru, F., Gurnett, D., Modolo, R., Barabash, S., Lundin, R., 2009. Ionospheric storms on Mars: Impact of the corotating interaction region. Geophys. Res. Lett. 36, L01105. doi:10.1029/2008GL036559.

Duru, F., Gurnett, D.A., Morgan, D.D., Modolo, R., Nagy, A.F., Najib, D., 2008. Electron densities in the upper ionosphere of Mars from the excitation of electron plasma oscillations. J. Geophys. Res. 113, A07302. doi:10.1029/2008JA013073.

Espley, J.R., Cloutier, P.A., Brain, D.A., Crider, D.H., Acuña, M.H., 2004. Observations of low-frequency magnetic oscillations in the martian magnetosheath, magnetic pileup region, and tail. J. Geophys. Res. 109, A07213. doi:10.1029/2003JA010193.

Espley, J.R., Farrell, W.M., Brain, D.A., Morgan, D.D., Cantor, B., Plaut, J.J., Acuña, M.H., Picardi, G., 2007. Absorption of MARSIS radar signals: Solar energetic particles and the daytime ionosphere. Geophys. Res. Lett. 34, L09101. doi:10.1029/2006GL0288.

Gurnett, D.A., Bhattacharjee, A., 2005. Introduction to Plasma Physics. Cambridge University Press, Cambridge, United Kingdom.

Gurnett, D.A., and 11 colleagues, 2005. Radar soundings of the ionosphere of Mars. Science 310, 1929–1933.

Gurnett, D.A., and 13 colleagues, 2008. An overview of radar soundings of the martian ionosphere from the Mars Express spacecraft. Adv. Space Res. 41 (9), 1335–1346.

Leblanc, F., Luhmann, J.G., Johnson, R.E., Chassefiere, E., 2002. Some expected impacts of a solar energetic particle event at Mars. J. Geophys. Res. 107 (A5), SIA5. doi:10.1029/2001JA900178.

Mendillo, M., Withers, P., Hinson, D., Rishbeth, Henry, Reinisch, B., 2006. Effects of solar flares on the ionosphere of Mars. Science 311, 1135–1138.

Morgan, D.D., Gurnett, D.A., Kirchner, D.L., Huff, R.L., Brain, D.A., Boynton, W.V., Acuña, M.H., Plaut, J.J., Picardi, G., 2006. Solar control of radar wave absorption by the martian ionosphere. Geophys. Res. Lett. 33, L13202. doi:10.1029/2006GL026637.

Morgan, D.D., Gurnett, D.A., Kirchner, D.L., Fox, J.L., Nielsen, E., Plaut, J.J., 2008. Variation of the Martian ionospheric electron density from Mars Express radar soundings. J. Geophys. Res. 113, A09303. doi:10.1029/2008JA013313.

Nielsen, E., Morgan, D.D., Kirchner, D.L., Plaut, J.J., Picardi, G., 2007. Absorption and reflection of radio waves in the martian ionosphere. Planet. Space Sci. 55, 864–870.

Patterson, J.D., Armstrong, T.P., Laird, C.M., Detrick, D.L., Weatherwax, A.T., 2001. Correlation of solar energetic protons and polar cap absorption. J. Geophys. Res. 106, 149–163.

Picardi, G., and 34 colleagues, 2005. Radar soundings of the subsurface of Mars. Science 310, 1925–1928.

Plaut, J.J., and 24 colleagues, 2007. Subsurface radar sounding of the south polar layered deposits of Mars. Science 316, 5821. doi:10.1126/science.1139672.

Tsurutani, B.T., and 13 colleagues, 2006. Corotating solar wind streams and recurrent geomagnetic activity: A review. J. Geophys. Res. 111, A07S01. doi:10.1029/2005JA011273.

Vignes, D., Mazelle, C., Rème, H., Acuña, M.H., Connerney, J.E.P., Lin, R.P., Mitchell, D.L., Cloutier, P., Crider, D.H., Ness, N.F., 2000. The solar wind interaction with Mars: Location and shapes of the bow shock and the magnetic pile-up boundary from the observation of the MAG/ER experiment onboard Mars Global Surveyor. Geophys. Res. Lett. 27 (1), 49–52.

Wang, J.-S., Nielsen, E., 2004. Solar wind modulation of the martian ionosphere observed by Mars Global Surveyor. Ann. Geophys. 22, 2277–2281.

Winningham, J.D., and 45 colleagues, 2006. Electron oscillations in the induced martian magnetosphere. Icarus 182, 360–370.

Withers, P., Mendillo, M., 2005. Response of peak electron densities in the martian ionosphere to day-to-day changes in solar flux due to solar rotation. Planet. Space Sci. 53, 1401–1418.